Lasers in Manufacturing Conference 2015

Capillary geometries during welding of metals observed with X-ray technique and calculated using a ray-tracing tool and a finite volume program treating heat diffusion and fluid flow

Peter Berger*, Andreas Heider, Meiko Boley, Daniel Förster

Institut für Strahlwerkzeuge (IFSW), Universität Stuttgart, Pfaffenwaldring 43, 70569 Stuttgart, Germany

Abstract

To understand and to predict the seam properties in deep-penetration laser welding, it is important to know the shape of the capillary. High-speed X-ray videography is an adequate technique to observe the average shape and the temporal development of the capillary. Other observation methods use transparent materials in front of the workpiece or instead of the metallic workpiece. Capillary features, which are observed by X-ray technique and which are typical for different materials, will be compared. The investigated materials have in common, that the lower part of the capillary often shows a different behavior compared to the upper part. For example the lower part shows more fluctuations can be more inclined or more often exhabits bulging on the rear side.
To understand the observed phenomena better, calculations can be performed. The calculations presented here use a model which combines a ray-tracing module with a finite volume program treating heat conduction and fluid flow. In this model the surface of the capillary is defined by a large number of triangles which are rearranged after each time step in order to fulfill mass, momentum, and energy balance. The structure of this surface is perfectly suited for fast ray tracing. With this model some interesting features of the capillary shape and of the temporal behavior observed during the experiments could be described although momentum transfer within the vapour was not included in the model.

Keywords: laser welding, capillary geometry, modeling, simulation, X-ray technique

* Corresponding author. Tel.: +49-711-685-66843; fax: +49-711-685-66842.
E-mail address: berger@ifsw.uni-stuttgart.de.

1. Introduction

In laser welding of metals one distinguishes between conduction-mode welding and deep-penetration welding. While in the first mode, the laser beam heats the surface of the workpiece to a temperature between melting and vaporization point, in the second case the maximum temperature reaches vaporization temperature. In this case a capillary is formed by the recoil pressure of the evaporating metal and the laser beam can penetrate deep into the workpiece enabling deep and narrow weld seams. The shape of this capillary, its surface structure and its temporal fluctuations together with the material properties and the characteristics of the laser beam determine the amount of absorbed energy and its special and temporal distribution. The seam properties and the quality of the weld are strongly influenced by these factors. However, the methods to investigate the capillary geometry are limited.

Therefore, in the next chapter a short overview is given how heat-source models and the calculation of the beam propagation in the capillary can contribute to this topic. In the following chapter observation methods will be introduced briefly together with some actual findings and an open question. Finally results from a numerical model, which treats the hydrodynamics of the melt flow and the heat conduction in the workpiece together with the laser beam propagation and absorption, will be discussed.

2. Distribution of the absorbed power within the capillary

First analytical and numerical calculations of the weld bead shape were performed in the 1930s and 1940s. Rosenthal, 1935 was one of the first who treated this topic. The sources he developed were as simple as possible. A moving point source at the surface of the workpiece was used to model the heat-conduction welding and a traveling line source was used for the deep-penetration welding, which is typical for electron-beam and laser-beam welding. Many authors have extended the scope of his model. Cline and Anthony, 1977 e.g. described a line source with finite length. These models have in common that the capillary shape is a result of the model. In the original line-source model, the capillary is almost circular for low welding velocities, for high velocities, however, it gets long and narrow, Fig. 1 a). This shape seems to be unrealistic compared to experimental investigations, although the capillary gets elongated with increasing welding velocity in the experiments also.

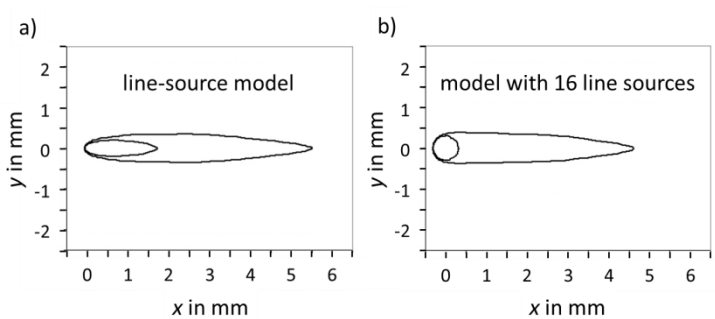

Fig. 1. Weld pool shape of a deep-penetration welding of iron at a welding velocity of 20 m/min with a power per depth of 3.57 kW/mm (a) using the line-source model; (b) using a model with 16 line sources; the power per depth of each individual line source was chosen in a way that a circular vaporization isotherm results with a radius of 0.3 mm

If the shape of the capillary ought to have a certain form, a combination of the elementary heat sources mentioned above can be used. In the right part of Fig. 1 e.g. sixteen line sources have been used. The power of each source was chosen individually in order to generate an almost circular capillary. A perfect cylindrical shape can be obtained if an infinite number of line sources is used. Noller, 1983 has presented an analytical solution for this specific model. In a more general way, a number of point sources can be used to generate almost any capillary shape desired, Chang, 2000. In all models mentioned above it is usually assumed that the capillary shape is represented by the surface which is at evaporation temperature.

Yet it is not clear whether the rear side of the capillary is at evaporation temperature or not. At least at high welding velocities the temperature at the rear side of the capillary seems to be below vaporization temperature. If the temperature distribution within the capillary is to be calculated, in a first step the light propagation and absorption within the capillary has to be determined space- (and time-) resolved. In principle, this can be done by treating physical optics using Maxwell's equations. However, due to the small time step and high special resolution that is needed for the calculation, with actual available computers only very small volumes can be simulated. An example can be seen in Fig. 2.

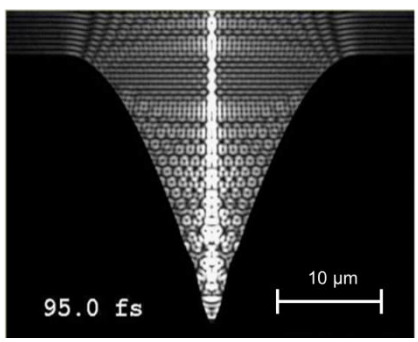

Fig. 2. Light propagation and absorption in a small capillary, calculated numerically using Maxwell's equations, Ruf, 2004

Courtois et al, 2014 applied this technique to capillaries of sizes realistic in high-power laser-beam welding by using a wavelength, that is much larger compared to the real laser beam, and by adapting the complex refraction index n, k in a way that enables realistic absorption values. But mostly the ray-tracing algorithm is used for large capillaries. Among the first, who modeled the deep-penetration welding process by use of the ray-tracing algorithm, were Beck and Dausinger, 1989 and Kaplan, 1994.

Unfortunately, for all these models, except the point- and line-source model, the capillary shape has to be known and prescribed as a boundary condition.

3. Observation of the capillary shape

Up to now, there is only a limited number of techniques to investigate the capillary shape. Arata et al., 1978 used a sandwich structure consisting of a metallic workpiece and a glass plate in his so called "direct luminous observation method". During the high speed observation a heat-proof glass was in contact with the side of a specimen and the electron beam was impinged along the boundary between glass and specimen.

Several experiments have been carried out since then using only transparent material instead of a metallic specimen. Glass, plastics and ice have been used as well as liquid materials such as water and oil.

Tong and Giedt, 1969 were probably the first who used a flashing high-voltage source to generate a pulsed beam of X-rays which was passed through the workpiece during the actual welding process so that

the size and shape of the capillary could be recorded on X-ray film. Weber et al., 1972 used the emitted X-ray radiation resulting from the process zone to record images of the capillary on X-ray sensitive film material. Starting with Arata et al., 1978 Arata's group published numerous investigations performed by X-ray technique. In recent years several investigations have been performed at the IFSW using a micro-focus X-ray source and an image converter which allow high speed recording with high spatial resolution. In Figs. 3 and 4 there are examples of steel, aluminum and bronze as specimen. While the capillaries, which are observed during welding of steel, are typically straight and slender, aluminum, bronze and copper often show kinked and/or bulged capillaries. In case of aluminum the bulging frequently results in a pore generation. In case of bronze the bulged shape seems to be more stable and in case of copper the bulging sometimes results in an ejection of melted material.

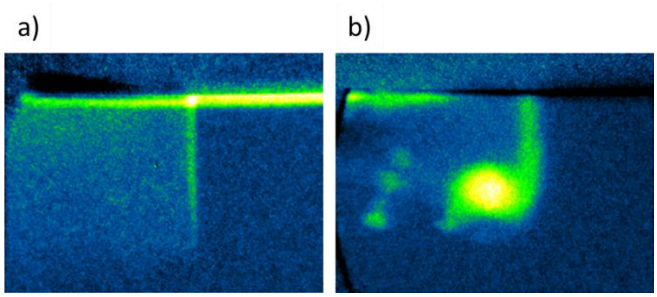

Fig. 3. Single frames from an high-speed video recorded during the welding process of a) stainless steel with a solid state laser with a power of 5000 W at 3 m/min, b) aluminum with a solid state laser with a power of 3000 W at 3 m/min

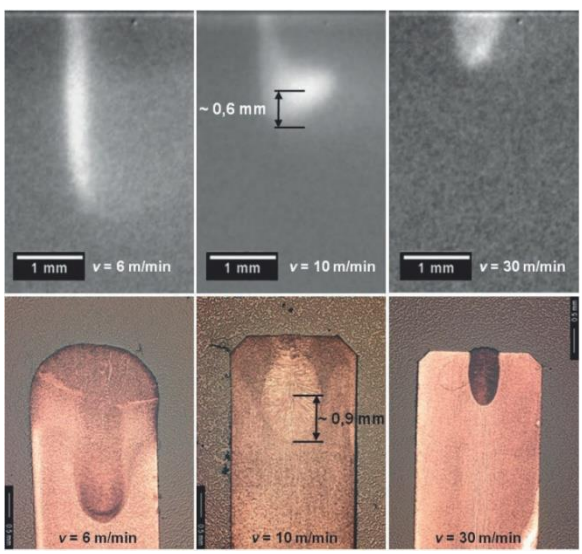

Fig. 4. Upper part: Single frames from an high-speed video recorded during the welding process of CuSn6 bronze using a solid state laser with a power of 5000 W and a focal diameter of 150 µm; below: corresponding cross sections; from left to right: 6 m/min, 10 m/min and 30 m/min, Heß, 2012

A possible explanation for the occurrence of the kinked shape and for the bulging is a strong localized evaporation at the capillary front close to the kink. The momentum generated by the evaporation is transferred by the vapor jet to the rear side and pushes the melt backwards, compare Fig. 5. A second explanation seems also plausible. If the capillary front bends more and more with increasing velocity, more and more light is reflected to the rear side causing evaporation directly at the rear capillary wall. The recoil pressure generated by evaporation at the capillary's rear wall should push the melt easily backwards.

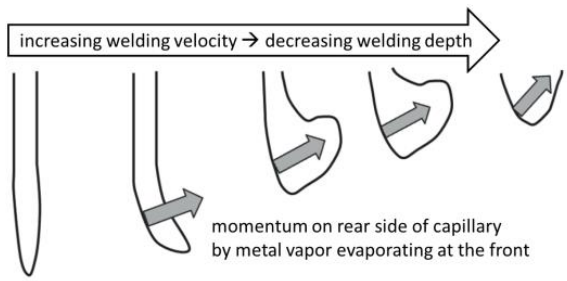

Fig. 5. Change of capillary shape when increasing the welding velocity, Heß, 2012

4. Calculation of capillary shapes

The ray-tracing models mentioned above (Beck and Dausinger, 1989 and Kaplan, 1994) used a heat conduction module together with the ray-tracing module. The second module calculates the energy absorbed at the capillary surface, the first module the amount of energy which is conducted into the workpiece. Assuming that the energy losses caused by evaporation are small, both flows of energy can be balanced. Modifying the capillary's surface in a proper manner until the heat flows are balanced at each point yields the capillary's shape. Using a reasonable beam profile, this leads to a stable and smooth capillary shape. In those first models the pressure generated by the evaporating surface was not calculated.

By introducing a third module, which calculates the recoil pressure and balances the dynamic pressure of the melt with this recoil pressure, usually the surface of the capillary gets wavy and no stable solution can be found, see e.g. Fabbro and Chouff, 2000, Ki et al., 2002 and Courtois et al, 2014.

In this paper, a similar model was used to investigate whether the bulging of the capillary can be explained by the reflection of light and evaporation directly at the capillary's rear side. In this model the surface of the capillary is defined by a large number of triangles which are rearranged after each time step in order to fulfill mass, momentum, and energy balance. The structure of this surface is perfectly suited for fast ray tracing. A finite volume method was used to solve the heat conduction in the solid and liquid phase and the heat convection caused by the melt flow, OpenCFD Ltd, 2014. For the results presented here, the material properties of steel were used (viscosity 0.005 Pas, density: 7000 kg/m³, heat conductivity 45 W/mK, specific heat 750 J/kgK, latent heat of melting 292 kJ/kg, solidus temperature 1775 K, liquidus temperature 1815 K, vaporization temperature 3300 K, latent heat of vaporization 6360 kJ/kg, gradient of surface tension 0.00045 N/mK, surface tension at melting temperature 1.7 N/m, coefficient of the density variation 0.00002 1/K, complex index of refraction (2.59, 4.87). The recoil pressure is proportional to the power density absorbed at the surface but not conducted to the bulk. The vapor inside the capillary is not treated with the consequence that no momentum is transferred from one side of the capillary to the other. Fig 6 shows the

temperature distribution on the upper surface and in the symmetry plane of the specimen. In Fig. 7 some capillary shapes calculated with that model are presented.

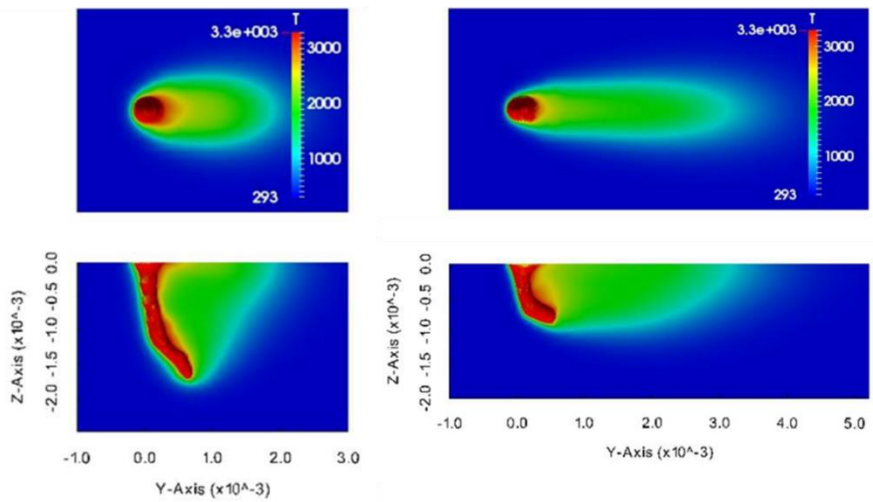

Fig. 6. Temperature distribution in the workpiece, laser power 3000 W, focal diameter 300 µm, approximately 10 ms after start of welding, a) at 10 m/min, b) at 20 m/min, Buck, 2014

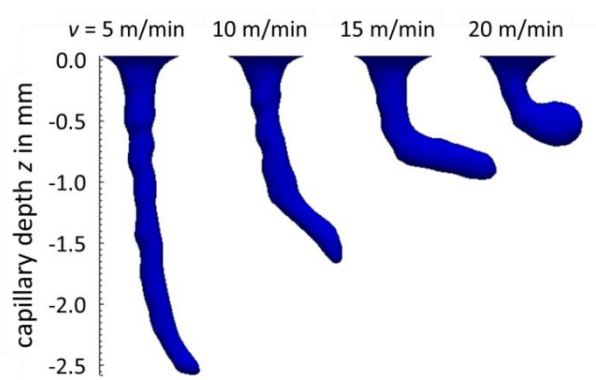

Fig. 7. Capillary shapes calculated with a model using ray-tracing, heat transport by conduction and convection in the melt as well as a pressure balance between the dynamic pressure of the melt and the recoil pressure, the gas phase within the capillary is not treated, therefore, no momentum transfer occurs from one side of the capillary to the other, Buck, 2014

The kinks observed in the outcomes of the model result from light reflections at the wavy surface of the capillary front. While in the upper part only a small amount of light reaches the rear capillary wall, in the lower part the amount of energy absorbed by the rear capillary wall is large enough to case strong deformations of the capillary. The momentum transfer by the vapor jet impinging on the rear wall, which is not treated here, might enhance this effect.

References

Rosenthal, D., 1935. “Etude théorétique du régime thermique pendant la soudure a l’arc,” 2eml Congres National des Sciences, Brucelles.

Cline, H.E., Anthony, T.R., 1977. Heat treating and melting material with a scanning laser or electron beam. Journal of Applied Physics 48, p. 3895-3900.

Noller, F., 1983. “The stationary shapes of vapor cavity and molten zone on eb-welding,” 3rd International Conference on Welding and Melt, Electrons and Laser Beam, p. 89-97.

Chang, C.-L., 2000. Berechnung der Schmelzbadgeometrie beim Laserstrahlschweißen mit Mehrfokustechnik, Herbert Utz Verlag · Wissenschaft, München.

Ruf, A., 2004. Modellierung des Perkussionsbohrens von Metallen mit kurz- und ultrakurzgepulsten Lasern, Herbert Utz Verlag · Wissenschaft, München.

Courtois, M., Carin, M., Le Masson, P., Gaied, S., Balabane, M., 2014. A complete model of keyhole and melt pool dynamics to analyze instabilities and collapse during laser welding, Journal of Laser applications, 26, p. 042001.

Beck, M., Dausinger, F., 1989. “Modelling of Laser Deep Welding Processes”. European Scientific Laser Workshop ’89. Lisbon, Portugal, p. 201-216.

Kaplan, A., 1994. A Model of Deep Penetration Laser Welding Based on Calculation of the Keyhole Profile. Journal of Physics D: Applied. Physics 27, p. 1805-1814.

Tong, H., Giedt, W. H., 1969. Radiographs of the Electron Beam Welding Cavity, Review of Scientific Instruments, 40 (10), p. 1283-1285.

Weber, C. M., Funk, E. R., McMaster, R. C., 1972. Penetration Mechanism of Partial Penetration Electron Beam Welding, Welding Journal, 51, 02, p. 90-96.

Arata, Y., Nabegata, E., Iwamoto, N., 1978. Tandem Electron Beam Welding (Report-II), Transactions of the JWRI, 7(2), p. 233-243.

Boley, M., Berger, P., Webster, P. J. L., Weber, R., Van Vlack, C., Fraser, J., Graf, T., 2013. „Investigating the Weld Depth Behaviour Using Different Observation Techniques: X-Ray, Inline Coherent Imageing and Highspeed Observation During Welding Ice,” 32nd International Congress on Applications of Lasers and Electro-Optics (ICALEO). Miami, USA, paper #105.

Heß, A., 2012. Vorteile und Herausforderungen beim Laserstrahlschweißen mit Strahlquellen höchster Fokussierbarkeit, Herbert Utz Verlag · Wissenschaft, München.

Fabbro, R., Chouff, K., 2000. Dynamical description of the keyhole in deep penetration laser welding, Journal of Laser Applications 12, No. 4, p. 142-148.

Ki, H., Mohanty, P.S., Mazumder, J., 2002. Modeling of Laser Keyhole Welding: Part I. Mathematical Modeling, Numerical Methodology, Role of Recoil Pressure, Multiple Reflections, and Free Surface Evolution, Metallurgical and Materials Transactions A, 33A, p. 1817.

Ki, H., Mohanty, P.S., Mazumder, J., 2002. Modeling of Laser Keyhole Welding: Part II. Simulation of Keyhole Evolution, Velocity, Temperature Profile, and Experimental Verification. Metallurgical and Materials Transactions A, 33A, p. 1831.

Buck, P., 2014, Kopplung von Absorptionsrechnungen mit transienter Wärmeleitung und Fluiddynamik zur Simulation von Lasermaterialbearbeitungsprozessen, master thesis, IFSW, University of Stuttgart.

OpenCFD Ltd, 2014. User guide. http://www.openfoam.org/docs/user/index.php.